

Mechanism of linear and nonlinear optical effects of KDP and urea crystals

Zheshuai Lin, Zhizhong Wang, and Chungtian Chen

Technical Institute of Physics and Chemistry, Beijing Center for Crystal Research and Development, Chinese Academy of Sciences, P.O. Box 2711, Beijing, 10080, People's Republic of China

Ming-Hsien Lee

Department of Physics, Tamkang University, Tamsui, Taipei 251, Taiwan

(Received 16 July 2002; accepted 6 November 2002)

First-principles calculations of the linear and nonlinear optical properties of KH_2PO_4 (KDP) and $\text{CO}(\text{NH}_2)_2$ are presented. The calculations are an extension of methods we developed earlier and applied to borate crystals. Electronic band structure obtained from a pseudopotential method is input to the calculation. For two crystals considered, the resulting indices of refraction, birefringence, and nonlinear optical coefficients are in good agreement with experiments. The origin of nonlinear effects has been explained through real-space atom-cutting analysis. For KDP, the contributions of PO_4 groups to second-harmonic generation effect are dominant, and the hydrogen bonds contribute much more to birefringence. For both KDP and urea, the contributions from the virtual electron process to nonlinear optical responses are dominant. © 2003 American Institute of Physics.

[DOI: 10.1063/1.1533734]

I. INTRODUCTION

The very first materials to be used and exploited for their nonlinear optical (NLO) and electro-optic (EO) properties were potassium dihydrogen phosphate (KDP) and ammonium dihydrogen phosphate (ADP). They were used in the early experiments in nonlinear optics and they are still widely used in nonlinear optical devices. They also continue to be popular as electro-optic materials because they are readily grown in useful sizes with good optical homogeneity. The nonlinear coefficients of other nonlinear optical crystals show considerable variation from crystal to crystal, which is not the case for the KDP group, there is better agreement among the reported values for their nonlinear coefficients than for other materials. The electro-optic and nonlinear optical properties of KDP and its isomorphs were reviewed by Eimerl.¹ The crystal structure of KDP belongs to the acentric orthorhombic point group $mm2$ in its ferroelectric phase below 123 K, and above this temperature belongs to the acentric tetragonal point group $\bar{4}2m$ in the paraelectric phase.² The unit cell of KDP having $I\bar{4}2d$ space group³ is shown in Fig. 1(a). In the KDP structure, fundamental PO_4 units are bonded together through the H atoms in the hydroxy groups of the O's of PO_4 . The structure of KDP is not complicated, however, the spontaneous polarization in the material does not provide a complete description of acentricity. Levine has applied the bond charge model calculations to arbitrary space group, and in particular to KDP.⁴ Reasonable agreement with experimental data was obtained with extrapolation of empirically determined effective parameters. A few studies of *ab initio* calculations for KDP have been published. In 1992 Hao *et al.*⁵ calculated and discussed the potential energy surface for the O–H···O bond in KDP. In 1993 Silvi and his colleagues investigated the electronic structure and the proton transfer potential energy curve by a periodic Hartree–Fock quantum chemical method.⁶ In a very recent publica-

tion, Zhang *et al.*⁷ reported an *ab initio* study of the electronic and structural properties of the ferroelectric transition in KDP. To our knowledge no first-principle calculation of nonlinear optical coefficient of KDP has appeared in literature.

As discussed in the review of Halbout and Tang,⁸ crystalline urea was among the first organic materials to find an application in nonlinear optics, specifically phase-matched second-harmonic generation (SHG) in the ultraviolet region. From a fundamental point of view, this crystal is interesting because it is among the simplest organic crystals that have second-harmonic responses. The unit cell of urea crystal with $P\bar{4}21m$ space group symmetry is shown in Fig. 1(b). Urea is also hydrogen bonded, which leads to enough delocalization, yet it has strong localized features such as π electrons in the carbonyl groups which contribute significantly to nonlinear response. Levine and Allan have reported a first-principles calculation for the urea crystal and pointed out that nonlinear local-field corrections are important.⁹ Earlier, Morrell and co-workers performed a complete neglect of differential overlap/spectroscopic (CNDO/S) calculation on urea crystal.¹⁰ An earlier complete neglect of differential overlap (CNDO) method is also used to calculate the dielectric constant.¹¹

In recent years, we have reviewed the calculation methods of the second-harmonic generation (SHG) based on first principles and suggested an improved calculation formula.^{12,13} The calculation requires input describing the electronic band structure, which we obtained from CASTEP,¹⁴ a total energy calculation computer software package. We have used our method to successfully calculate linear and nonlinear optical (NLO) responses of a series of important NLO crystals such as BBO,¹³ LBO, CBO and CLBO,¹⁵ BIBO,¹⁶ KBBF,¹⁷ NaNO_2 ,¹⁸ and SrBe_3O_4 .¹⁹ The origins of the SHG effects of these crystals were clearly explained

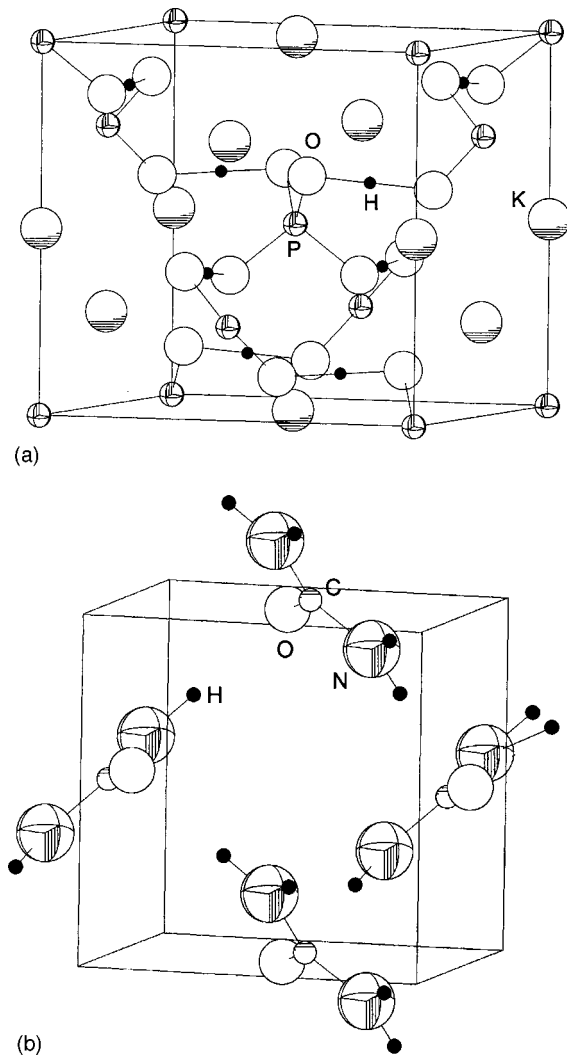


FIG. 1. Unit cell of KDP and urea crystals. (a) KDP, (b) urea.

by using atom-cutting analysis method. This analysis method isolates the contribution of individual atoms or groups of atoms by removing spatial localized wave functions from the evaluation.

The goal of this work is to calculate the electronic structures and the linear and nonlinear optical parameters of KDP and urea crystals from first-principles quantum mechanics and to give an explanation of the origin of the optical responses. Results of the calculations on KDP and urea crystals show that our calculation method is adequate for KDP and urea crystals.

II. COMPUTATIONAL METHOD

The plane-wave pseudopotential total energy software package CASTEP¹⁴ is used for solving the electronic and band structure. These results are applied to the calculations of linear and nonlinear optical properties of the crystals. The theoretical basis of CASTEP is the density functional theory (DFT).²⁰ The optimized pseudopotentials in the Kleinman–Bylander form for C, N, O, P, K, and H^{21–23} allow us to use a small plane-wave basis set without compromising the accuracy required by our study. For systems with bond elec-

trons in which the effects of the free charge carriers can be neglected, the nonlinear optical properties of a materials are mainly determined by the magnitudes of the static limit of the SHG coefficients $\chi^{(2)}(0)$, which plays the most important role in the applications of SHG crystals. We adopt the representation of the second-order susceptibility

$$\chi^{\alpha\beta\gamma} = \gamma^{\alpha\beta\gamma}(\text{VE}) + \chi^{\alpha\beta\gamma}(\text{VH}) + \chi^{\alpha\beta\gamma}(\text{two bands}), \quad (1)$$

where $\chi^{\alpha\beta\gamma}(\text{VE})$ and $\chi^{\alpha\beta\gamma}(\text{VH})$ denote the contributions from virtual-electron processes and virtual-hole processes, respectively, and $\chi^{\alpha\beta\gamma}(\text{two bands})$ gives the contribution from two band (TB) processes to $\chi^{(2)}$. The formulas for calculating $\chi^{\alpha\beta\gamma}(\text{VE})$, $\chi^{\alpha\beta\gamma}(\text{VH})$, and $\chi^{\alpha\beta\gamma}(\text{two bands})$ are as follows:

$$\chi^{\alpha\beta\gamma}(\text{VE}) = \frac{e^3}{2\hbar^2 m^3} \sum_{vcc'} \int \frac{d^3k}{4\pi^3} P(\alpha\beta\gamma) \text{Im}[p_{vc}^\alpha p_{cc'}^\beta p_{c'v}^\gamma] \times \left(\frac{1}{\omega_{cv}^3 \omega_{v'c}^2} + \frac{2}{\omega_{vc}^4 \omega_{c'v}^4} \right), \quad (2)$$

$$\chi^{\alpha\beta\gamma}(\text{VH}) = \frac{e^3}{2\hbar^2 m^3} \sum_{vv'c} \int \frac{d^3k}{4\pi^3} P(\alpha\beta\gamma) \text{Im}[p_{vv}^\alpha p_{v'c}^\beta p_{cv}^\gamma] \times \left(\frac{1}{\omega_{cv}^3 \omega_{v'c}^2} + \frac{2}{\omega_{vc}^4 \omega_{cv'}^4} \right), \quad (3)$$

and

$$\chi^{\alpha\beta\gamma}(\text{two bands}) = \frac{e^3}{\hbar^2 m^3} \sum_{vc} \int \frac{d^3k}{4\pi^3} P(\alpha\beta\gamma) \times \frac{\text{Im}[p_{vc}^\alpha p_{cv}^\beta (p_{vv}^\gamma - p_{cc}^\gamma)]}{\omega_{vc}^5}. \quad (4)$$

Here, α , β , and γ are Cartesian components, v and v' denote valence bands, and c and c' denote conduction bands. $P(\alpha\beta\gamma)$ denotes full permutation. The band energy difference and momentum matrix elements are denoted as $\hbar\omega_{ij}$ and p_{ij}^α , respectively.

The structural parameters of KDP crystal with $I\bar{4}2d$ space group symmetry are taken from the work of West³ and are $a=b=7.43$ Å and $c=6.97$ Å. In a primitive cell there are four KDP molecules. Crystalline urea belongs to $P\bar{4}21m$ space group. Its geometry is taken from the work of Guth *et al.*²⁴ and are $a=b=5.572$ Å and $c=4.686$ Å. In a primitive unit cell there are two urea molecules.

III. RESULTS AND DISCUSSIONS

In the following we separately give the calculated results and discussions for KDP and urea crystals.

A. KDP

1. Energy bands of KDP

The calculated energy bands along the line of high symmetry points in the Brillouin zone are illustrated in Fig. 2. The total density of states (DOS) and partial DOS (PDOS) projected on the constitutional atoms are plotted in Fig. 3.

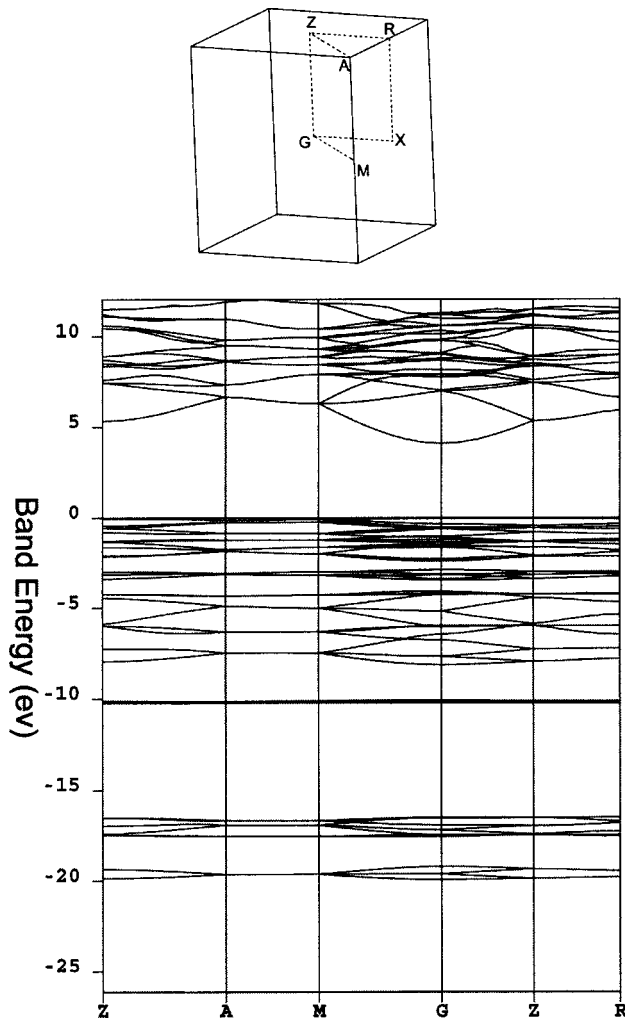


FIG. 2. Band structure of KDP crystal.

Both the top of the valence band (VB) and the bottom of the conduction band (CB) are at *G* (gamma point). The direct band gap of 4.178 eV is obtained, which is significantly smaller than the experimental value of 7.12 eV (~174 nm).²⁵ The calculated band gaps are usually smaller than the corresponding experimental ones with density functional theory. To fit the measured absorption edge, the energy scissors operator is commonly employed to shift up all conduction bands.^{26,27} For the calculation of KDP the scissors energy 3.00 eV was applied. Assuming that the r_{mn} matrix elements are unchanged, the momentum matrix elements should be renormalized regarding the change of the Hamiltonian in a way given by

$$p_{nm} \rightarrow p_{nm} \frac{\omega_{nm} + \Delta/\hbar(\delta_{nc} - \delta_{mc})}{\omega_{nm}}, \quad (5)$$

where the subscript *c* in Kroneckers represents conduction band, and the Δ factor restricts the correction to pairs of band only involving one valence-band and one conduction-band state.

From Figs. 2 and 3 it can be seen that the band structure is separated into three subregions. The lower one is located

below -15 eV. It is composed of the O 2*p* and the P 3*s* orbital with a little mixing H 1*s*. The middle subregion is the valence band which is very flat. The VB is mostly from the O 2*p* and the P 3*p* with small contribution from H and K orbitals. The *K*-*p*-derived state is located about -10 eV. The upper subregion is the conduction band which consist mainly of the O 2*p* and the P 3*p* with small contribution from H and K orbitals.

2. Linear optical response of KDP

It is known that the refractive indices can be obtained theoretically from the dielectric function. The imaginary part of the dielectric function can be calculated with the matrix elements which describe the electronic transitions between the ground state and the excited states in the crystal considered. The formula is given by

$$\text{Im}[(\epsilon_{ij}(\omega))] = \frac{e^2}{\pi m^2 \hbar} \sum_{mn} \int dk \frac{f_{nm} p_{nm}^i p_{mn}^j}{\omega_{nm}^2} \delta(\omega_{nm} - \omega), \quad (6)$$

where $f_{nm} = f_n - f_m$, and f_n, f_m are Fermi factors. The real part of the dielectric function is obtained by the Kramers-Kronig transform.²⁸

In Table I we listed theoretical refractive indices and birefringence of KDP. The calculated refractive indices of KDP are in good agreement with experimental values. The calculated birefringence $\Delta n = 0.042$ is in reasonable agreement with the measured value $\Delta n = 0.035$.

To investigate the respective contributions of different ionic groups, we employed the real-space atom-cutting method.¹³ With this method the contribution of ion *A* to the *n*th-order susceptibility, denoted as $\chi^{(n)}(A)$, is obtained by cutting all ions except *A* from original wave functions, i.e., $\chi^{(n)}(A) = \chi_{\text{All ions except A are cut}}^{(n)}$. In a previous paper we found that the charge density around the cation is spherical.¹³ Thus we first choose the cutting radius of K as 1.40 Å. Following the rule of keeping the cutting spheres of the cation and O in contact and not overlapped, we choose the cutting radii of O and P atoms to be 1.10 and 1.25 Å, respectively. The atom-cutting analysis results are also given in Table I. The contributions to refractive indices of the PO₄ group dominate, but birefringence contribution of the PO₄ group, having symmetrical tetrahedral structure, is only 0.0247. In the BPO₄ calculation (theoretical $\Delta n = 0.005$) we also found that the symmetrical tetrahedral structures have small contribution to birefringence. Furthermore we calculated the contribution to birefringence of the H₂PO₄ group and obtained $\Delta n = 0.0495$. This shows that hydrogen bond contribution to birefringence is almost double that of the PO₄ group. The result of atom-cutting analysis indicates that K⁺ has almost nothing to do with the birefringence. This result is in accordance with our previous conclusions for LBO, CBO, CLBO, and other materials.¹⁵⁻¹⁷

3. The nonlinear optical response of KDP

It is known that the second order susceptibility $\chi^{(2)}$ is a double of the SHG coefficient d_{ij} . According to the Kleinman symmetry relation²⁹⁻³¹ there is only a single indepen-

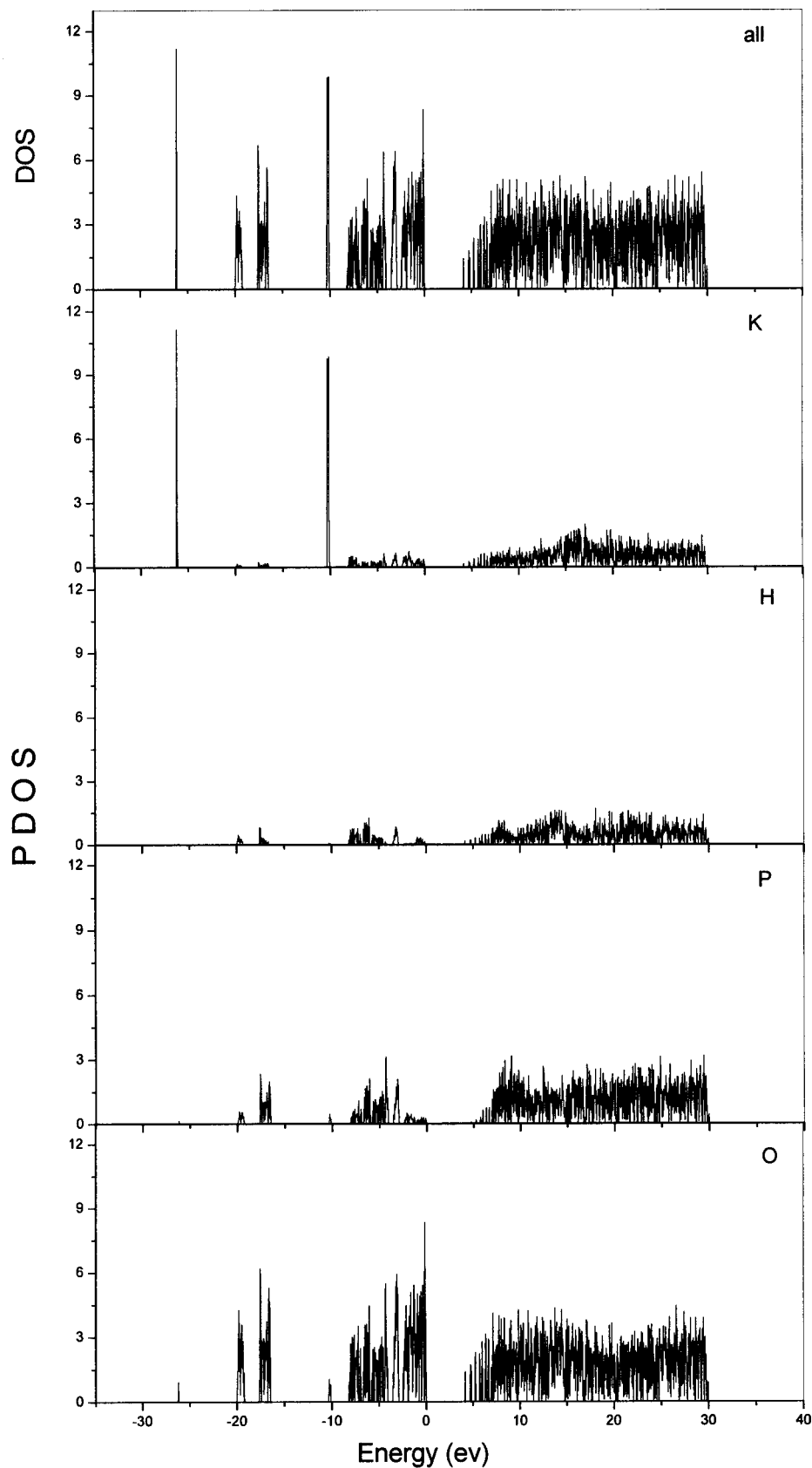


FIG. 3. DOS and PDOS plot of KDP crystal.

dent SHG coefficient $d_{14}=d_{36}$ for KDP with $\bar{4}2m$ point group symmetry. The calculated nonlinear coefficient of KDP crystal is 0.42 pm/V which is in good agreement with the experimental value of 0.39 pm/V.²⁵ Results of the atom-

cutting method applied to the calculation of the SHG coefficients are also given in Table I. Comparison of $d_{36}(\text{H}_2\text{PO}_4)$ and $d_{36}(\text{PO}_4)$ shows that hydrogen bond has small contributions to the SHG effect. Apparently, the anionic groups

TABLE I. Comparison of the calculated and experimental values of refractive indices, birefringence and SHG coefficient, together with atom-cutting analysis results for KDP crystal.

	n_x	n_y	n_z	Δn	d_{36} (pm/V)
Expt. ^a	1.495 35	1.495 35	1.460 41	0.035	0.39
Calc.	1.5518	1.5518	1.5104	0.0415	0.42
Atom-cutting analysis					
PO ₄	1.4649	1.4649	1.4402	0.0247	0.417
H ₂ PO ₄	1.4977	1.4977	1.4482	0.0495	0.421
K	1.1125	1.1125	1.1112	0.0013	0.004

^aReference 25.

(PO₄)⁻³ contribute approximately 99% to SHG coefficients, and cation K⁺ has nothing to do with the SHG effect.

To investigate the respective influence of the various transitions on the optical responses of the KDP and urea crystals, the contributions of different transitions to SHG effect are calculated. The results are given in Table II. The contribution from the virtual electron (VE) process to the SHG effect closely approaches the experimental value. On

TABLE II. The contributions of SHG coefficients of different transitions for KDP and urea (unit: pm/V).

Crystals	KDP	Urea
d_{36} (Calc.)	0.42	1.043
Contributions		
VE	0.406	1.083
VH	0.010	-0.04
TB	0.000	0.00

the other hand, the contribution from the virtual hole (VH) process to the SHG effect are 2.4% and 3.8% for KDP and urea, respectively.

B. Urea crystal

1. Energy bands of urea

The calculated energy bands along lines of high symmetry and the total density of the states (DOS) of crystalline urea are given in Fig. 4. The partial DOS projected on the constitutional atoms is shown in Fig. 5. Both the top of the

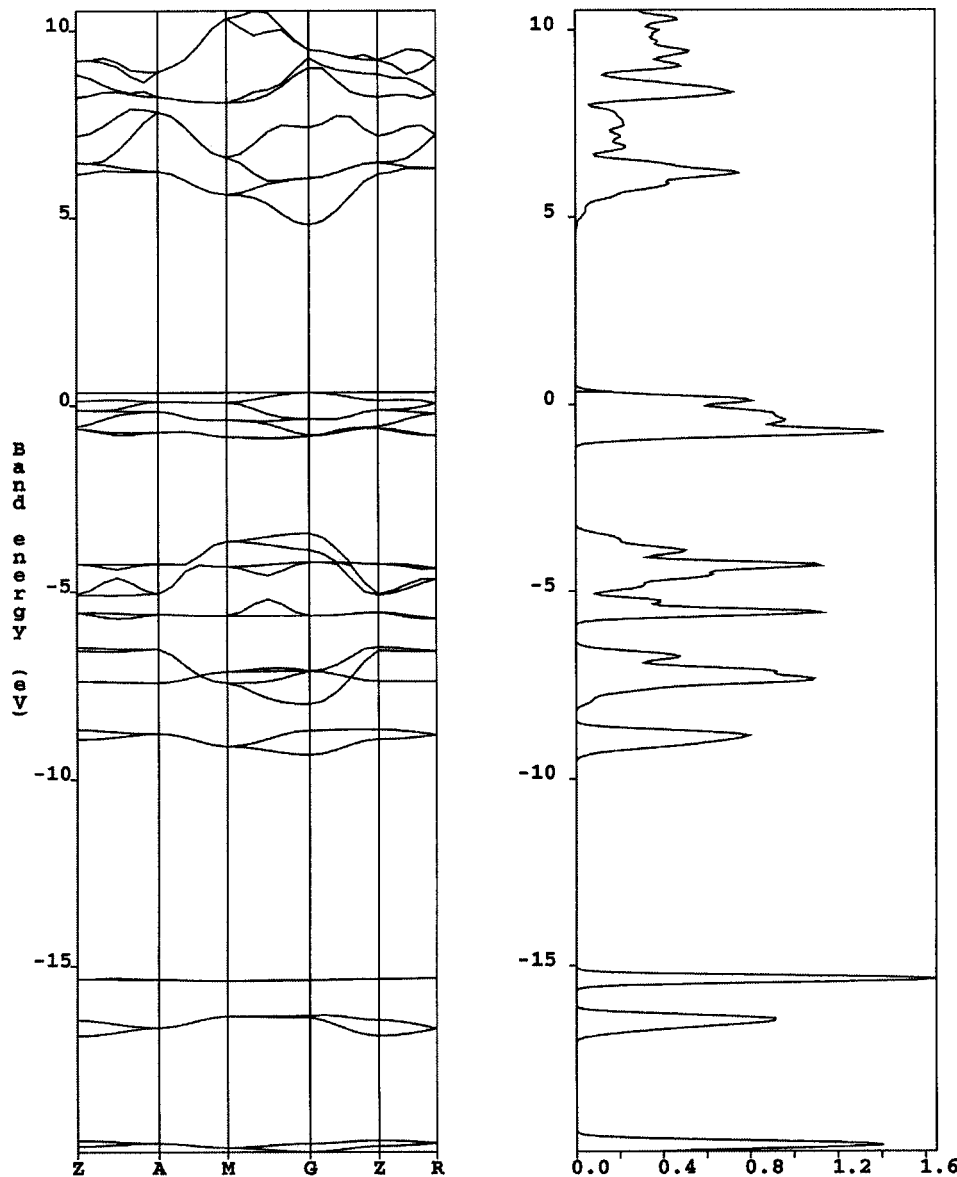


FIG. 4. Band structure and DOS plot of urea. k points are the same as that in Fig. 2.

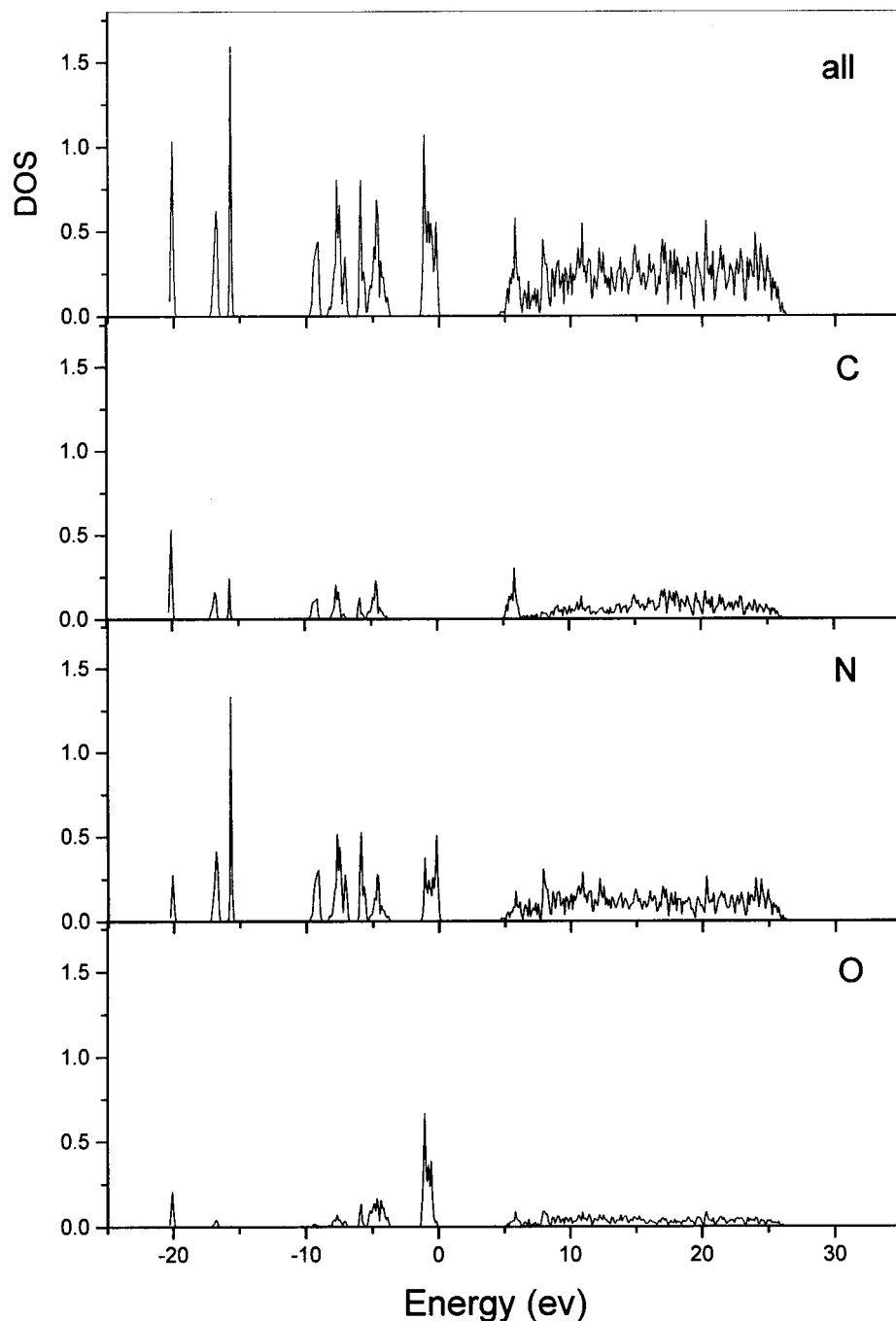


FIG. 5. PDOS plot of urea crystal.

VB and the bottom of the CB are at point G (gamma point). The direct band gap of 4.27 eV has been obtained. This value is smaller than the experimental value of 6.18 eV (~ 200 nm). The scissors energy 1.91 eV was used to fit the measured values. The energy bands are flat and not seriously dispersive. This is a typical characteristic of small intermolecular interactions for molecular crystals. Both energy band and DOS figures show the entire energy bands are divided into three subregions. The lowest subregion is below -15 eV and is composed of three isolate sharp spike peaks. The peak centered at -20 eV is the mixture of C, N, and O $2s$ orbitals. The other two peaks are composed of C and N $2s$ orbitals. The middle subregions are valence bands (VB) from 0 to -9.0 eV and consist of two parts. The top of the VB consists of C and O $2p$ orbitals. The peaks from -4 to -9 eV mostly

come from $2p$ orbitals of C, O, and N. The upper subregion is the conduction band (CB), which shows the apparent interaction between C and N valence orbitals. These interactions between orbitals of C, N, and O (bonding) reveal that the framework OCN_2 in urea molecule is an entity.

2. Linear optical response of urea

For urea crystal the calculated refractive indices and birefringence are listed and compare with experimental values in Table III. The theoretical values are in good agreement with the experimental data. Both theoretical and experimental birefringence values are $\Delta n = 0.1$.

The calculated charge density contour is shown in Fig. 6. This charge density map indicates that the $\text{CO}(\text{NH}_2)_2$ is an

TABLE III. Calculated and experimental refractive indices, birefringence and atom-cutting analysis results for urea crystal.

	λ (nm)	n_x	n_y	n_z	Δn
Expt.	1064	1.4720	1.4720	1.5817	0.1132
Calc.	1064	1.5037	1.5037	1.6247	0.1210
Contributions of transition between VB and CB bands of respective groups					
VB	CB				
CO	CO	1.3463	1.3463	1.4615	0.1152
CO	NH ₂	1.2670	1.2670	1.2981	0.0311
NH ₂	NH ₂	1.3974	1.3974	1.4269	0.0322
NH ₂	CO	1.3028	1.3028	1.3328	0.0300

entity. That is to say, we cannot cut any cation or anion from the molecule, so we should treat it as a whole. The contributions of different types of electron transitions are given in Table III. Apparently, all transitions contribute to the linear optical response, but the birefringence of urea crystal originates mainly from the transitions between VB and CB of the conjugated group CO. The other transitions in urea crystal contribute little to the anisotropy.

3. The nonlinear optical response of urea

Levine and Allan have pointed out that for the case of urea, it is necessary to invoke Kreinman symmetry,^{29–31} which is appropriate far from resonance. Urea crystal belongs to point group $\bar{4}2m$. There are two possible SHG coefficients for this point group, and Kreinman symmetry requires $d_{123}=d_{312}$. In compressed notation this is $d_{14}=d_{36}$. The SHG coefficients have been also calculated from the band energies and wave functions using the computational formulas (1)–(4). The calculated SHG coefficients at the static limit $d_{14}=1.04$ pm/V are given in Table IV. The agree-

TABLE IV. Comparison of experimental and calculated SHG coefficients of urea from this work and others.

	λ (nm)	d_{14} (pm/V)
CNDO ^a	1064	0.89
LDA (no local field) ^b	∞	2.1
LDA ^b	∞	1.1
Present work	∞	1.044
Expt. crystal ^c	1060	1.2 \pm 0.1
Expt. crystal ^d	600	1.3 \pm 0.3

^aReference 11.

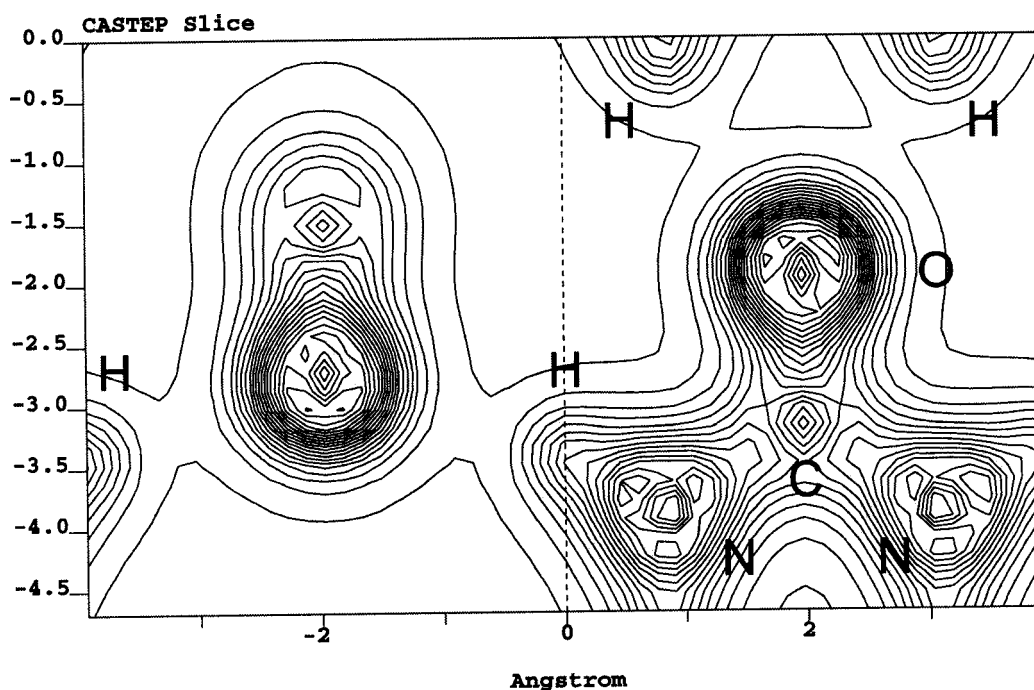
^bReference 6.

^cReference 32.

^dReference 30.

ment between the theoretical and experimental values is good. For comparison in Table IV we have listed other theoretical investigations of the SHG coefficients of crystalline urea. The theoretical value of semiempirical CNDO calculation does not agree as well with the experimental one because the intermolecular interaction was not included.¹¹ Levine and Allan⁹ reported the LDA calculation results without and with the local field, and the latter was found in good agreement with the experimental measurements. Present results are consistent with the Levine and Allen calculation that included the local field.

To investigate the respective influence of the various transitions on the optical responses of the urea crystal, the contributions of different transitions to SHG effect were calculated. The results are given in Table II. We found the contribution from the virtual electron process to the SHG effect closely approaches the experimental value. On the other hand, the contribution from the virtual hole process to the SHG effect is only -0.04 pm/V, but its sign is opposite to that of the virtual electron process. In our previous investi-

FIG. 6. Charge density contour plot on the CO(NH₂)₂ plane of urea crystal.

gation on the mechanism for linear and nonlinear optical effects of β -BaB₂O₄ (BBO) crystal, we have pointed out that generally the virtual electron process contributes more to the total response than the virtual hole process.¹³ However, in the case of BBO crystal the contribution to the large component d_{22} from virtual hole process is about 30% of the total nonlinear optical response. This is unlike the case of GaAs for which the contribution of the VH process is always negative and is smaller than that of the VE process by over an order of magnitude. This difference is based on the different structures of the energy bands of zinc-blende semiconductors and borate crystals. The energy gaps of semiconductors are much smaller than those of the borate crystals. The organic urea crystal is different from both the zinc-blende semiconductors and borates. For urea crystal the top of the VB is very flat and the band gap is large. The dominant contribution to the SHG value is given by the VE process. In addition the transitions related to the CO group contribute more than 70% to the overall SHG effect of urea.

IV. CONCLUSION

Ab initio electronic band-structure calculations have been carried out using the CASTEP package to study the optical properties of KDP and urea. Our investigations are summarized as follows:

(i) The electronic and band structures of KDP and urea have been obtained. The band structures of both KDP and urea are typical of an insulating system with larger energy gaps. The DOS and PDOS figures reveal the compositions of each energy band. For KDP the top of VB and the bottom of the CB are mostly from the O 2*p* and P 3*p* orbitals with small contribution from H and K orbitals. For urea the top of the VB consists of C and O 2*p* orbitals and the bottom of the CB shows an apparent interaction between C and N valence orbitals with a little contribution from O orbitals.

(ii) The linear and nonlinear optical coefficients have been obtained for two crystals from the wave functions and band energies. The calculated refractive indices, birefringences, and SHG coefficients are in all good agreement with experimental values. The real-space atom-cutting method applied to KDP reveals the respective contributions of cation K⁺ and anions PO₄³⁻ and H₂PO₄⁻ to optical responses. The results show that the contributions to linear and nonlinear optical responses from both PO₄³⁻ and H₂PO₄⁻ are comparable. However, the latter contributions to birefringence is about double of the former. This indicates that anions PO₄³⁻ dominate SHG coefficient of KDP and hydrogen bonds contribute approximately about 50% of the birefringence. For both KDP and urea crystals the contributions of different transitions to the SHG coefficients are investigated. The processes of virtual electrons are dominant and virtual hole processes can be neglected for two considered crystals.

Above-mentioned conclusions confirm that the CASTEP DFT pseudopotential package and our calculation formula for SHG are suitable for dealing with the relationship between the microscopic structure and the SHG coefficients of KDP, urea and other analogous materials. In addition, the

real-space atom-cutting method can reveal the origins of the optical responses for NLO crystals. We believe that further applications of the methodology used in present work may elucidate the origins of the optical effects, both linear and nonlinear, in other NLO crystals and help us to find and design new NLO crystals more efficiently.

ACKNOWLEDGMENTS

This work was supported by the Chinese National Key Research Project. Support in computing facilities from the Computer Network Information Center is gratefully acknowledged. M.H.L. thanks funding support from NSC 90-2102-M-032-011.

¹D. Eimerl, *Ferroelectrics* **72**, 95 (1987).

²S. H. Wemple and M. DiDomenico, Jr., *Appl. Solid State Sci.* **3**, 263 (1972).

³J. West, *Z. Kristallogr.* **74**, 306 (1930).

⁴B. F. Levine, *Phys. Rev. B* **7**, 2600 (1973).

⁵Y. G. Hao, S. X. Y. Sun, and N. S. Dalal, *Ferroelectrics* **132**, 165 (1992).

⁶B. Silvi, Z. Latajka, and H. Ratajczak, *Ferroelectrics* **150**, 303 (1993).

⁷Q. Zhang, F. Chen, N. Kioussis, S. D. Demos, and H. B. Radousky, *Phys. Rev. B* **65**, 024108 (2001).

⁸J. M. Halbout and C. L. Tang, in *Nonlinear Optical Properties of Organic Molecules and Crystals*, edited by D. S. Chemla and J. Zyess (Academic, New York, 1998), p. 385.

⁹Z. H. Levine and D. C. Allan, *Phys. Rev. B* **48**, 7783 (1993).

¹⁰J. A. Morrell, A. C. Albrecht, K. H. Levin, and C. L. Tang, *J. Chem. Phys.* **71**, 5063 (1979).

¹¹E. N. Svendsen, C. S. Willand, and A. C. Albrecht, *J. Chem. Phys.* **83**, 5670 (1985).

¹²Z. S. Lin, J. Lin, Z. Z. Wang *et al.*, *J. Phys.: Condens. Matter* **13**, R369 (2001).

¹³J. Lin, M. H. Lee, Z. P. Liu, C. T. Chen, and C. J. Pickard, *Phys. Rev. B* **60**, 13380 (1999).

¹⁴CASTEP 3.5 program developed by Molecular Simulation Inc., San Diego, CA, 1997.

¹⁵Z. S. Lin, Z. Z. Wang, C. T. Chen, and M. H. Lee, *Phys. Rev. B* **62**, 1757 (2000).

¹⁶Z. S. Lin, Z. Z. Wang, C. T. Chen, and M. H. Lee, *J. Appl. Phys.* **90**, 5585 (2001).

¹⁷Z. S. Lin, Z. Z. Wang, C. T. Chen, S. K. Chen, and M. H. Lee, *Chem. Phys. Lett.* (in press).

¹⁸Z. S. Lin, Z. Z. Wang, and C. T. Chen, *Acta Phys. Sin.* **50**, 1145 (2000).

¹⁹Z. S. Lin, Z. Z. Wang, C. T. Chen, H. T. Yang, and M. H. Lee, *J. Chem. Phys.* **117**, 2809 (2002).

²⁰R. G. Parr and W. T. Yang, *Density Functional Theory of Atom-Molecules* (Oxford University Press, Oxford, 1989).

²¹A. M. Rappe, K. M. Rabe, E. Kaxiras, and J. D. Joannopoulos, *Phys. Rev. B* **41**, 1227 (1990).

²²J. S. Lin, A. Qtseish, M. C. Payne, and V. Heine, *Phys. Rev. B* **47**, 4174 (1993).

²³M.-H. Lee, J.-S. Lin, M. C. Payne, V. Heine, V. Milman, and S. Crampin (unpublished).

²⁴H. Guth, G. Heger, S. Klein, W. Treutmann, and C. Scherlinger, *Acta Crystallogr., Sect. B: Struct. Crystallogr. Cryst. Chem.* **34**, 1624 (1978).

²⁵V. G. Dimitriev, G. G. Gurzadyan, and D. N. Nikogosyan, *Handbook of Nonlinear Optical Crystals*, 2nd revised ed. (Springer, Berlin, 1977).

²⁶R. W. Godby, M. Schluter, and L. J. Sham, *Phys. Rev. B* **37**, 10159 (1988).

²⁷C. S. Wang and B. M. Klein, *Phys. Rev. B* **24**, 3417 (1981).

²⁸J. E. Sipe and E. Ghahramani, *Phys. Rev. B* **48**, 11705 (1993).

²⁹D. A. Kleinman, *Phys. Rev.* **126**, 1977 (1962).

³⁰D. Baurele, K. Betzler, H. Hesse, S. Kaplan, and P. Loose, *Phys. Status Solidi A* **42**, K119 (1977).

³¹K. Betzler, H. Hesse, and P. Loose, *J. Mol. Struct.* **47**, 393 (1978).

³²J.-M. Halbout, S. Blit, W. Donaldson, and C. L. Tang, *IEEE J. Quantum Electron.* **QE-15**, 1176 (1979).